



Received April 7, 2020, accepted April 14, 2020, date of publication April 20, 2020, date of current version May 4, 2020.

Digital Object Identifier 10.1109/ACCESS.2020.2988725

# Coefficient of Voltage Energy Efficiency

PIOTR GNACIŃSKI<sup>1</sup> , (Member, IEEE), JANUSZ MINDYKOWSKI<sup>1</sup>, (Senior Member, IEEE),  
MARCIN PEPLIŃSKI<sup>1</sup>, (Member, IEEE), TOMASZ TARASIUK<sup>1</sup>, (Member, IEEE),  
JOSE D. COSTA<sup>2</sup>, MÁRIO ASSUNÇÃO<sup>2</sup> , LUIS SILVEIRA<sup>2</sup>,  
VADYM ZAKHARCHENKO<sup>3</sup>, ALLA DRANKOVA<sup>3</sup>,  
MYKOLA MUKHA<sup>3</sup>, (Member, IEEE),  
AND XIAO-YAN XU<sup>4</sup>

<sup>1</sup>Department of Ship Electrical Power Engineering, Gdynia Maritime University, 81-225 Gdynia, Poland

<sup>2</sup>Department of Maritime Engineering, Escola Náutica Infante D. Henrique, 2770-058 Paço de Arcos, Portugal

<sup>3</sup>Electrical Engineering Department, National University "Odessa Maritime Academy", 65029 Odessa, Ukraine

<sup>4</sup>Electrical Engineering Department, Shanghai Maritime University, Shanghai 201306, China

Corresponding author: Piotr Gnaciński (p.gnacinski@we.umg.edu.pl)

This work was supported by the International Association of Maritime Universities through the research Project under Grant 20190202.

**ABSTRACT** The reduction of greenhouse gas emissions is a major contemporary challenge. This has prompted the requirements concerning energy efficiency for ships, among other things. Improvement in efficiency of ship operations could be achieved by reducing unnecessary power consumption by induction motors. Specifically, the occurrence of power quality disturbances, such as frequency and voltage deviations, voltage unbalances, and voltage harmonics, can cause an extraordinary increase in the power losses occurring in induction motors, as well as an unnecessary increase in the output power. Furthermore, excessive power quality disturbances are often interconnected with failures of on-board equipment, and in extreme cases, these may even pose a threat to safety at sea. Consequently, strict power quality monitoring of on-board microgrids can also contribute to improving safety while afloat. In this study, a dedicated tool for power quality monitoring is proposed, namely the *coefficient of voltage energy efficiency*, which has a value proportional to the power losses occurring in induction motors under power quality disturbances.


**INDEX TERMS** Energy efficiency, induction motors, marine technology, power systems, power quality.

## I. INTRODUCTION

The reduction of greenhouse gas emissions is a major contemporary challenge. To this end, in 2012, the *International Convention for the Prevention of Pollutions from Ships (MARPOL Annex VI)* imposed specific requirements concerning energy efficiency for ships. Among other factors, new ships are required to attain an appropriate value of the *Energy Efficiency Design Index (EEDI)*. Further, a *Ship Energy Efficiency Management Plan (SEEMP)* should be developed for each vessel. In practice, various operations for reducing energy consumption should be planned and executed, and their implementation should be monitored and self-evaluated appropriately (*Resolution MEPC.213(63) of the International Maritime Organization*). A possible solution for improving the efficiency of ship operations could be the reduction of unnecessary power consumption by induction motors, the efficiency of which is significantly dependent

on the quality of the supply voltage. The appearance of power quality disturbances, such as frequency and voltage deviations, voltage unbalances, and voltage waveform distortions (for example, harmonics) may cause as much as a 50 percent increase in the power losses inside an induction motor. Furthermore, power quality disturbances may lead to ineffective utilisation of the mechanical energy produced by the motors. That is, power quality disturbances (within the levels permitted by the rules of ship classification societies) may cause an increase of up to approximately 5% in the rotational speed of the induction motors. This is put into context by recognising that the mechanical power consumed by fans and centrifugal pumps is proportional to the cubed rotational speed. Consequently, for the disturbances permitted in ship systems, the power on the shaft may even increase by approximately 15% above the design level. In many cases, such a power increment would be deemed unnecessary.

The *coefficient of voltage energy efficiency* ( $c_{vee}$ ), which is proposed in this study, may provide an appropriate tool for the assessment and monitoring of such undesirable effects.

The associate editor coordinating the review of this manuscript and approving it for publication was Lin Zhang .

The value of this coefficient will indicate whether the induction motors operate efficiently or exhibit excessive power losses. An appropriate value could be recommended for attainment by new ships, as with the EEDI. Moreover, the coefficient could be used for implementations in the SEEMP. If its value should reach an unsuitable level during the operation of a ship's motors, appropriate measures would be implemented to improve the voltage quality. In the authors' experience, the appearance of significant power quality disturbances is often interconnected with the malfunctioning of various types of on-board equipment, such as blown fuses and harmonic filters. In extreme cases, these disturbances may even threaten ship safety. If the power quality disturbances and the coefficient reach a critical level, an ad hoc solution could be to switch on an additional generator. This would entail an undesirable increase in the prime mover's specific fuel consumption, but it would also increase the safety level, and a by-product would be an increase in the energy efficiency of the induction motors. Therefore, additional monitoring of the power quality can influence ship safety. It is also worth mentioning that the proposed new coefficient could likewise be used in offshore plants.

## II. POWER QUALITY DISTURBANCES IN SHIP POWER SYSTEMS

### A. FEATURES OF SHIPBOARD MICROGRID AND POWER QUALITY DISTURBANCES

A ship power system differs significantly from other microgrids as well as large land power systems. It is characterised by specific design solutions and operational conditions. The main features of such a system are the limited capacity of generation and the power of a singular receiver, compared with the power of the generators installed on-board. As a result, significant variations of supply voltage quality are observed. Voltage deviations, unbalance and harmonic distortions have increasingly become the norm rather than the exception in modern shipboard microgrids. Among others, this is due to the comparatively high number of nonlinear loads, which usually consist of inverter-driven induction motors, various equipment malfunctions, and environmental conditions. In particular, wind and waves can lead to notorious frequency fluctuations. The phenomenon can be attributed to the use of shaft generators on-board, or the increasing usage of electric propulsion.

A shaft generator [1], which is a specific type of generator driven by propulsion machinery, is a particular technical solution that is applied only in ship power systems. It may supply a power system directly or via power electronic converters. Consequently, the operation of a shaft generator may lead to significant voltage waveform distortions [1] or to variations in the voltage frequency in the case of shaft generators supplying the power system directly, which is due to possible changes in the rotational speed of the main engine. Besides the effects of shaft generators, sea waves also impact the electric drives of the ship propulsion, causing torque

variations in the ship propeller. As a result, the load in the shipboard power system fluctuates. A further complication arises from the commonly used droop control running method for active power distribution between generators running in parallel, which causes significant quasi-periodic frequency fluctuations related to load variations as well, sometimes reaching a few percent of the rated frequency. An example of angular frequency variations in the fundamental voltage component under rough sea is shown in [2]. A basic configuration of a ship power system with three diesel-driven generators is presented in Fig. 1.

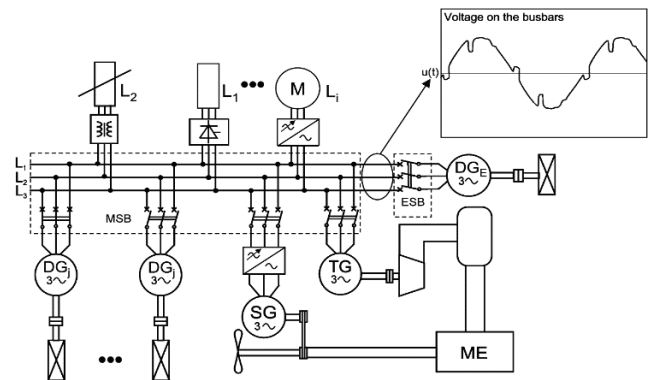


**FIGURE 1.** Generic diagram of a ship power plant [3]. SG: shaft generator; TG: generator driven by a turbine supplied with steam produced in a waste-heat boiler connected to the main engine (ME); DG: diesel engine-driven generators;  $L_1 \dots L_n$ : loads.

In summary, the features of the ship microgrid may lead to a deterioration of the power quality. In extreme cases, excessive power quality disturbances may even result in malfunctioning of the entire power system and pose a serious threat to safety at sea.

### B. REQUIREMENTS CONCERNING POWER QUALITY IN SHIP POWER SYSTEMS

Appropriate rules and standards have been introduced to protect each element of a ship power system against the detrimental effects of power quality disturbances [4]. The power quality requirements of individual ship classification societies, as well as of the International Association of Ship Classification Societies, are generally in accordance with the standard of the International Electrotechnical Commission, *IEC 60092-101 Electrical installations in ships — Part 101: Definitions and general requirements* [4]. The standard [4] permits a frequency deviation of  $\pm 5\%$  and a voltage deviation within the range of  $-10\%$  to  $+6\%$ , among others. Additionally, a voltage unbalance (which is understood as the difference between the highest and lowest line to line voltages) of  $3\%$  is accepted. Most ship classification societies also require that the total harmonic distortion (THD) of the voltage should not exceed  $8\%$ , and no single order harmonic distortion should exceed  $5\%$ .

The rules of ship classification societies and the standard [4] consider each power quality disturbance separately.

The cumulative impact of the disturbances on the power receivers, including the impact on the energy-efficient operation of the induction motors, is not taken into account. Therefore, it is necessary to develop a new power quality index, namely the *coefficient of voltage energy efficiency*.

### C. SELECTION OF APPROPRIATE POWER QUALITY INDEX

Various synthetic power quality indices and methods for power quality assessment are described in [5]–[12]. In [5], [8], [9], synthetic power quality factors were formulated on the grounds of a weighted sum of various power quality indices, like the voltage total harmonic distortion (VTHD), the current total harmonic distortion (ITHD), the percentage of current or voltage unbalance, and the sinus of the phase angle displacement between the fundamental current and voltage components. In [11], [12], power quality factors were proposed as amalgamations of various power quality indices, based on a fuzzy logic approach. Those factors could be useful for the rating of energy suppliers and the setting of penalty tariffs, among others. A neural network-based method of power quality assessment is shown in [10]. In [6], the authors propose a power quality index to assess the impact of voltage harmonics and voltage unbalance on the heating of an induction motor. Further, in [7], a synthetic power quality factor—*temperature coefficient of power quality*—dedicated to marine application was elaborated. Its value is proportional to the winding temperature of fully-loaded induction motors under power quality disturbances. The appropriate power quality index which we propose here, namely the *coefficient of voltage energy efficiency*, should take into account the effect of a lowered voltage quality on the increased power losses inside induction machines, and on the effective use of their output power. As mentioned previously, power quality disturbances may lead to an increase in the rotational speed of induction motors. Furthermore, the mechanical power consumed by fans and centrifugal pumps is proportional to the cubed speed. Consequently, for permitted disturbances in ship systems, the power on the shaft may even increase by approximately 15% above the design level. In many cases, such a power increment would be deemed unnecessary or even harmful (e.g., through an increase of pressure in some systems), but in other cases, the increase could be efficiently utilised. For example, owing to increased output power, certain motors are expected to operate for a shorter period than when working under the nominal supply. Detailed investigations into this issue are beyond the scope of this study, although this phenomenon (an unplanned increase in the output power) may be considered as generally undesirable and should be reflected by the proposed coefficient.

The disadvantageous effects of power quality disturbances on the energy-efficient operation of induction motors may include a decrease in the machine efficiency, an increase in the input power, or machine losses, among other factors. An increase in the load torque (for example, owing to an increase in the rotational speed under a parabolic load) is associated with an increase in the power losses inside a

machine. For a load close to its rated value, the power losses are roughly proportional to the squared load torque. The choice of an increase in the input power of the induction motors as a measure of energy efficiency, exhibits a significant disadvantage: under certain power quality disturbances, the power consumed by an induction motor could be even less than that for the nominal supply (for example, under a decrease in the voltage frequency), but broadly understood efficiency can be low. Consequently, a power quality coefficient corresponding to the input power of the induction motors could be difficult to interpret. In contrast, the power losses occurring in induction motors provide an easy interpretation. An increase in power losses directly indicates that the induction motors are operating uneconomically. Additionally the value of power losses is significantly affected by an increase in the output power. Therefore, the power losses occurring in induction motors (as they relate to the value under nominal supply) are selected as the appropriate power quality index, the *coefficient of voltage energy efficiency*.

In the following sections, the derivation of the *coefficient of voltage energy efficiency* is presented. The derivation is based on the mathematical description of power losses in induction machines, the assumption of their generalised parameters, and the application of appropriate polynomial approximations to simplify the final formulae. The experimental verification of the value of the coefficient is discussed in a subsequent section.

## III. POWER LOSSES IN INDUCTION MOTORS AND POWER QUALITY DISTURBANCES

### A. INTRODUCTION

The *coefficient of energy efficiency* is proportional to the power losses occurring in induction cage motors under power quality disturbances. According to the standard IEC/EN 60034-2-1 *Rotating electrical machines – Part 2-1: Standard methods for determining losses and efficiency from tests (excluding machines for traction vehicles)* [13], the power losses and efficiency of induction motors can be determined by the summation of separate losses. The total power losses inside a motor ( $P_{tot}$ ) are obtained by adding the following components together: power losses in the stator windings ( $P_{sw}$ ), power losses in the rotor windings ( $P_{rw}$ ), power losses in the iron ( $P_{Fe}$ ), mechanical losses (friction and windage losses,  $P_m$ ), and stray load losses ( $P_{sll}$ ), as indicated in (1):

$$P_{tot} = P_{sw} + P_{rw} + P_{Fe} + P_m + P_{sll} \quad (1)$$

In practice, (1) can be rewritten using relative values by considering the power losses for any operating point in terms of a reference value. For example, considering the power losses for the nominal supply and a given load torque, (1) can be computed as:

$$P_{tot} = w_{sw}p_{sw} + w_{rw}p_{rw} + w_{Fe}p_{Fe} + w_m p_m + w_{sll}p_{sll} \quad (2)$$

where  $p_{sw}$ ,  $p_{rw}$ ,  $p_{Fe}$ ,  $p_m$ , and  $p_{sll}$  are the relative values of the power losses in the stator, the power losses in the rotor windings, the power losses in iron, mechanical losses, and stray

losses, respectively, related to their values under reference working conditions, while  $w_{sw}$ ,  $w_{rw}$ ,  $w_{Fe}$ ,  $w_m$ , and  $w_{sl}$  denote the contributions of each component of the total power losses under those working conditions.

**B. POWER LOSSES IN WINDINGS**

**1) POWER LOSSES IN WINDINGS DUE TO THE FUNDAMENTAL CURRENT COMPONENT**

For any working point, the power losses in one winding can be recalculated as follows:

$$p_w = i_w^2 \frac{\vartheta_r + K_\vartheta}{\vartheta_{ref} + K_\vartheta} \quad (3)$$

where  $p_w$  is the value of the power losses in each winding of a stator and a rotor, relative to its reference value (for example, under nominal supply and for a given load);  $i_w$  is the current flowing through each winding, relative to its reference value;  $\vartheta_r$  is the real winding temperature;  $\vartheta_{ref}$  is the reference winding temperature, that is, the temperature determined for the reference value of the power losses; and  $K_\vartheta$  is a coefficient that is equal to 235 for copper and 225 for aluminium [13].

In practice, the determination of winding power losses requires knowledge of the RMS current as well as the temperature of the windings. The currents can be calculated on the basis of an equivalent circuit, as illustrated in Fig. 2, described in [7]. The equivalent supply voltage ( $u_{eq}$ ), relative to the nominal supply voltage, is defined as (4):

$$u_{eq} = u - x_s f i_{mref} i_m \quad (4)$$

In (4),  $u$  is the relative value of the fundamental voltage component, with reference to the rated voltage;  $i_{mref}$  is the ratio of the magnetising current to the stator current under reference working conditions;  $f$  is the relative frequency of the supply voltage, with reference to the nominal frequency;  $i_m$  is the relative magnetising current, which is understood as the ratio of the magnetising current at the working point to the magnetising current under the reference working conditions; and  $x_s$  is the relative value of the stator leakage reactance, described by:

$$x_s = \frac{\sqrt{3} X_s I_{s\_ref}}{U_{rat}} \quad (5)$$

where  $X_s$  is the stator leakage reactance;  $I_{s\_ref}$  is the RMS value of the stator current at the reference working point; and  $U_{rat}$  is the rated voltage.

The relative magnetising current (relative to the value under reference conditions) can be approximated as follows [7]:

$$i_m = \frac{\frac{u}{f}}{1 - k_{im} \left( \frac{u}{f} - 1 \right)} \quad (6)$$

where  $k_{im}$  is a coefficient depending on the machine properties.

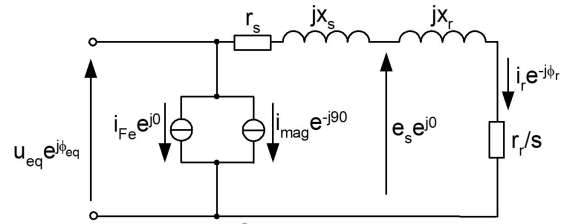


**FIGURE 2.** Equivalent circuit of an induction machine developed as discussed in [7];  $e_s$  is the relative rotor electromotive force,  $u_{neq}$  is the relative equivalent supply voltage and  $j$  is the imaginary unit.

The relative rotor current (relative to its value under reference working conditions) can be determined as follows [7]:

$$i_r = \sqrt{\frac{u_{neq}^2 - \frac{2r_s^* r_r^* t_e f}{s_{ref}} - \sqrt{u_{neq}^4 - \frac{4r_s^* r_r^* t_e f u_{neq}^2}{s_{ref}} - \frac{4r_s^{*2} x_z^{*2} f^4 t_z^2}{s_{ref}^2}}}{2r_s^{*2} + 2x_z^{*2} f^2}} \quad (7)$$

where

$$u_{neq} = \frac{u_{eq}}{u_{eq\_ref}}, r_s^* = \frac{r_s}{Z_{ref}}, r_r^* = \frac{r_r}{Z_{ref}}, x_z^* = \frac{x_s + x_r}{Z_{ref}} \quad (8a-d)$$

and

$$Z_{ref} = \sqrt{\left( r_s + \frac{r_r}{s_{ref}} \right)^2 + (x_s + x_r)^2}. \quad (8e)$$

In (7) and (8),  $s_{ref}$  is the slip under reference working conditions;  $t_e$  is the relative electromagnetic torque (relative to its value under reference working conditions); and  $r_s$ ,  $r_r$ , and  $x_r$  are the relative values of the stator winding resistance, rotor winding resistance, and rotor leakage reactance, respectively, which are defined analogously to the relative stator leakage reactance (5). The subscript  $ref$  corresponds to the reference working conditions (for the nominal supply and reference load torque).

For a machine driving a load of constant torque,  $t_e$  can be assumed to be equal to 1, whereas for a parabolic load torque (fan-type load), it can be estimated using the following expression [7]:

$$t_{par} = \frac{3AC + D + E - \frac{a_{ir} k_\varphi u_{neq}^2}{f} - Af}{5AC - 2Af + 3D - E - b_{ir} k_\varphi u_{neq} - r_s^* - B} \quad (9)$$

where

$$A = \alpha_r \frac{r_r^*}{s_{ref}}, \quad B = r_r^* (1 - \alpha_r), \quad C = 0.5 - \frac{s_{ref}}{2} \quad (10a-c)$$

$$D = C \frac{b_{ir} k_\varphi u_{neq} + r_s^*}{f}, \quad E = a_{ir} C \frac{k_\varphi u_{neq}^2}{f^2} \quad (10d-e)$$

$$k_\varphi = \frac{r_s + \frac{r_r}{s_{ref}}}{Z_{ref}}, \quad \alpha_r = \frac{K_\vartheta + 2\Delta\vartheta_{ref\_r} + \vartheta_0}{K_\vartheta + \Delta\vartheta_{ref\_r} + \vartheta_0} - 1 \quad (10f-g)$$

$$a_{ir} = 10 \frac{i_{r09} - 1}{i_{r09}}, \quad \text{and } b_{ir} = a_{ir} - 1 \quad (10h-i)$$

In (9) and (10),  $\vartheta_{ref\_r}$  is the reference temperature of the rotor windings;  $\vartheta_0$  is the ambient temperature;  $i_{r09}$  is equal to  $i_r$  determined for  $t_e = 1$ ;  $f = 1$ ; and  $u_{neq} = 0.9$ .

The relative stator current (relative to its value under reference working conditions) is expressed by [7]:

$$i_s = |i_{Fe} + i_{rref} i_r \cos\varphi_r + j(i_{mref} i_m + i_{rref} i_r \sin\varphi_r)| \quad (11)$$

where

$$\varphi_r = \text{atan} \left( \frac{s_{ref} x_r i_r^2}{r_r t_e} \right) \quad (12)$$

$i_{rref}$  is the ratio of the rotor current to the stator current under reference working conditions; and  $i_{Fe}$  is the current covering no-load losses, relative to the stator current under reference working conditions. For simplicity,  $i_{Fe}$  is assumed to be constant.

According to the authors' experience (for example, [7], [14]), additional machine heating under frequency and/or voltage variations may cause a considerable increase in the winding resistance, and consequently an increase in the current. Therefore, the resistance of the stator windings is re-calculated as follows:

$$r_s = \frac{\vartheta_0 + \Delta\vartheta_{ref} i_s^2 + K_\vartheta}{\vartheta_0 + \Delta\vartheta_{ref}} \quad (13)$$

where  $\Delta\vartheta_{ref}$  is the temperature increase (above the ambient temperature) of the stator windings under reference working conditions.

The above expression is based on the rough approximation that the increase in the temperature of the windings is proportional to the squared current. Thereafter, the current in the stator windings is computed again, in an iterative loop.

## 2) POWER LOSSES IN WINDINGS DUE TO CURRENT HARMONICS

Current harmonics can be estimated as follows (based on [15]):

$$i_h \approx \frac{u_h}{x_h} \quad (14)$$

where  $u_h$  is the voltage of a harmonic of the  $h^{\text{th}}$  order, related to the rated voltage; and  $x_h$  is the leakage reactance for the  $h^{\text{th}}$  harmonic.

The leakage reactance  $x_h$  can be assessed as follows (based on [15], [16]):

$$x_h = 2(x_s + x_r) \frac{f_h (f_h s_{h+}/h-)^{-0.16}}{f_{ref}} \quad (15)$$

where  $s_{h+}$  and  $s_{h-}$  are the slips for the positive-sequence and negative-sequence harmonics, respectively:

$$s_{h+} = \frac{h-1}{h} \quad (16)$$

and

$$s_{h-} = \frac{h+1}{h} \quad (17)$$

The influence of the variation of fundamental current harmonics on the leakage inductance is neglected. For a temperature equal to its reference value and an omitted skin effect in the stator windings, the relative increases in the power losses of the stator windings ( $p_{sw}$ ) and rotor windings ( $p_{srh}$ ) can be determined as follows (based on [7], [16]):

$$p_{sw} = \sum_{h=2}^{hmax} (i_h)^2 \quad (18)$$

and

$$p_{wrh} = \frac{1}{i_{rref}^2} \sum_{h=2}^{hmax} (i_h)^2 k_{rh} \quad (19)$$

where  $k_{rh}$  is a coefficient describing an increase in the resistance of a rotor cage owing to the skin effect. It can be estimated as follows (based on [15], [16]):

$$k_{rh} = 0.1Hc_r \sqrt{hf_{rat} s_{h+}/h-} + 1 - c_r \quad (20)$$

where  $c_r$  is a coefficient describing a bar shape;  $h$  is the harmonic order;  $f$  is the relative frequency of the supply voltage with reference to the rated frequency ( $f_{rat}$ ); and  $H$  is the useful slot depth [15] in cm.

For the purpose of this study, the useful slot depth  $H$  is assumed to be 2 cm and the coefficient  $c_r = 1$ . It should be noted that  $c_r = 1$  is an intermediate value between the values of  $c_r$  corresponding to various induction machines (based on [15]).

## 3) POWER LOSSES IN WINDINGS DUE TO A NEGATIVE-SEQUENCE CURRENT COMPONENT

Voltage unbalance generates the negative-sequence current, which can be calculated by applying the equivalent circuit presented in Fig. 3. If the magnetising reactance is neglected, the negative-sequence current  $i_-$  (relative to the stator current under reference working conditions) can be expressed by:

$$i_- = \frac{u_-}{\sqrt{\left(r_s + \frac{r_{r-}}{s_-}\right)^2 + (fx_s + fx_{r-})^2}} \quad (21)$$

where  $u_-$  is the negative-sequence voltage component;  $x_{r-}$  is the rotor reactance for the negative-sequence current and the frequency of the fundamental component being equal to the rated value, which can be estimated as approximately  $0.85 x_r$  [17];  $s_-$  is the slip for the negative-sequence current, equal to

$$s_- = 2 - s \approx 2 \quad (22)$$

and  $r_{r-}$  is the resistance of the rotor windings for the negative-sequence current:

$$r_{r-} = k_{r-} r_r \quad (23)$$

where  $k_{r-}$  is a coefficient describing an increase in the resistance of a rotor cage owing to the skin effect, which can be predicted using the dependency in (20) for  $h = 1$  and  $s_{h-} = 2$ .

The effect of the variation of the positive-sequence current on the leakage reactance is omitted.

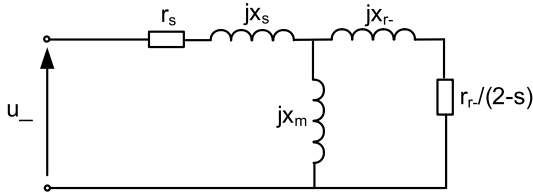


FIGURE 3. Equivalent circuit per phase of an induction machine for the negative-sequence current.

For a winding temperature equal to its reference value, the relative increase in the power losses in the stator and rotor windings caused by the negative-sequence current ( $p_{sw-}$  and  $p_{sr-}$ ) can be estimated as follows [7], [16]:

$$p_{sw-} = i_-^2 \tag{24}$$

$$p_{wr-} = \frac{1}{i_{rref}^2} k_r i_-^2 \tag{25}$$

#### 4) EFFECT OF WINDINGS TEMPERATURE ON OHMIC LOSSES

As mentioned previously, the power losses occurring in the windings depend on their temperature. For the actual winding temperature, the relative power losses in the stator and rotor windings (relative to their values under reference working conditions), namely  $p_{ws_r}$  and  $p_{wr_r}$ , respectively, can be expressed as:

$$p_{ws_r} = \frac{\vartheta_{rs} + K_\vartheta}{\vartheta_{ref\_s} + K_\vartheta} p_{sw\_ref} \tag{26}$$

and

$$p_{wr_r} = \frac{\vartheta_{rr} + K_\vartheta}{\vartheta_{ref\_s} + K_\vartheta} p_{rw\_ref} \tag{27}$$

where  $\vartheta_{rs}$  and  $\vartheta_{rr}$  are the real temperatures of the stator and rotor windings, respectively;  $\vartheta_{ref\_s}$  and  $\vartheta_{ref\_r}$  are the reference temperatures of the stator and rotor windings, respectively; and  $p_{sw\_ref}$  and  $p_{rw\_ref}$  are the relative power losses in the stator and rotor windings, respectively, determined for the reference temperatures:

$$p_{ws\_ref} = i_s^2 + p_{wsh} + p_{ws-} \tag{28}$$

$$p_{wr\_ref} = i_r^2 + p_{wrh} + p_{wr-} \tag{29}$$

In order to take into account the effect of the additional machine heating on the power losses in the windings, it can be roughly assumed that the real temperature increase (above the ambient temperature  $\vartheta_0$ ) of any winding is proportional to the total power losses. Consequently, the real temperature  $\vartheta_r$  of the stator or rotor windings can be estimated as:

$$\vartheta_r = \vartheta_0 + \Delta\vartheta_{ref} p_{tot\_r} \tag{30}$$

where  $p_{tot\_r}$  represents the total power losses (relative to the total power losses under reference working conditions) determined for the real temperatures of the stator and rotor windings and  $\vartheta_{rs}$  and  $\vartheta_{rw}$ ; and  $\Delta\vartheta_{ref}$  is the increase in the reference temperature (above the ambient temperature  $\vartheta_0$ ).

On the basis of equations (26) to (30), the following can be written:

$$p_{tot\_r} = w_{ws} p_{ws\_ref} [1 + \alpha_s (p_{tot\_r} - 1)] + w_{wr} p_{wr\_ref} [1 + \alpha_r (p_{tot\_r} - 1)] + p_{others} \tag{31}$$

where  $\alpha_s$  and  $\alpha_r$  are the dimensionless temperature coefficients of the stator and rotor winding resistances, respectively, defined by (10g) and (32) [16]:

$$\alpha_s = \frac{K_{\vartheta_s} + 2\Delta\vartheta_{ref\_s} + \vartheta_0}{K_{\vartheta_s} + \Delta\vartheta_{ref\_s} + \vartheta_0} - 1 \tag{32}$$

Further,  $p_{others}$  is the sum of the other components of the power losses (relative to the total power losses), which is considered in [13] as independent of the temperature:

$$p_{others} = w_{Fe} p_{Fe} + w_m p_m + w_{sll} p_{sll} \tag{33}$$

Following some mathematical transformations, the ratio of the total power losses in the windings, determined for the real and reference temperatures respectively, takes the form:

$$K_T = \frac{\alpha (p_{others} - 1) + 1}{1 - \alpha p_{wtot\_ref}} \tag{34}$$

where  $\alpha$  is an equivalent temperature coefficient for the stator and rotor windings:

$$\alpha = \frac{\alpha_s w_{sw} p_{sw\_ref} + \alpha_r w_{rw} p_{rw\_ref}}{w_{sw} p_{sw\_ref} + w_{rw} p_{rw\_ref}} \tag{35}$$

and  $p_{wtot\_ref}$  is the sum of the power losses in the stator and rotor windings (relative to the total power losses) for the reference temperature, which is defined as:

$$p_{wtot\_ref} = w_{sw} p_{sw\_ref} + w_{rw} p_{rw\_ref} \tag{36}$$

### C. IRON POWER LOSSES

#### 1) SUPPLY WITH SINUSOIDAL VOLTAGE

Under the assumption that the electromotive force occurring in the stator windings is proportional to the supply voltage and that hysteresis losses are significantly greater than eddy current losses, the approximate power losses in iron as a result of deviations in voltage and frequency can be recalculated as follows [7], [18]:

$$p_{Fesin} = u_1^x \left( \frac{p_h}{f} + p_{ec} \right) \tag{37}$$

where  $x$  is the Steinmetz coefficient; and  $p_h$  and  $p_{ec}$  are the ratios of the hysteresis and eddy current losses in the iron losses, respectively.

#### 2) SUPPLY WITH DISTORTED VOLTAGE

Under a distorted supply voltage, the power losses in iron can be assessed as follows (on the grounds of [7], [18]):

$$p_{Fe} = k_{Fedist} p_{Fesin} \tag{38}$$

where  $k_{Fedist}$  is a coefficient describing an increase in the iron power losses caused by voltage waveform distortions; its value may be determined by the following expression [18]:

$$k_{Fedist} = \eta_B^x p_h + \chi^2 p_h \tag{39}$$

where  $\chi$  is the ratio of the RMS voltage to the RMS value of the fundamental voltage component;  $\eta_B$  is the ratio of the peak flux for the sinusoidal supply to the peak flux for the supply with distorted voltage, which is equal to the ratio of the average rectified voltage to the average rectified fundamental voltage component; and  $x$  is the Steinmetz coefficient.

The ratio of the peak flux densities  $\eta_B$  can be evaluated as follows [19]:

$$\eta_B = \frac{1 + \frac{1}{u_1} \sum_{h=5,7,11,\dots}^{hmax} \frac{u_h}{h} \cos\phi_h}{u} \quad (40)$$

where  $\phi_h$  is a phase angle for each harmonic component.

It should be noted that even harmonics (divisible by 2) and harmonics divisible by 3 do not influence the flux peak value [19], and therefore these harmonics are omitted in the summation appearing in the above expression. Moreover, power quality analysers generally do not measure the phase angles of each harmonic. In practice, a simplified expression can be applied to evaluate the ratio  $\eta_B$  [19]:

$$\eta_B = \frac{1 + \frac{1}{u_1} \sum_{h=5,7,11,\dots}^{hmax} \frac{u_h}{h}}{u} \quad (41)$$

The effect of the voltage unbalance on the iron losses is omitted.

#### D. MECHANICAL LOSSES

Mechanical losses in induction cage motors are caused by friction in the bearings and windage. These losses can be recalculated as proportional to the square of the rotational speed [20]. For the purpose of this study, the relative mechanical losses  $p_m$  are assumed to obey a simple equality:

$$p_m = t_{par} \quad (42)$$

where  $t_{par}$  is the relative value of the parabolic load torque, according to (9), despite the fact that the squared relative rotational speed may slightly differ from  $t_{par}$  for a frequency reduction and a constant torque load.

#### E. STRAY LOSSES

Stray losses or high-frequency losses result from space harmonics in the air gap flux, slot leakage flux, and overhang leakage flux, among others [21], [22]. Stray losses are categorised as no-load and load stray losses. For the purpose of this study, the no-load stray losses are included in the iron losses. Stray load losses contain various components [22], which are usually of an eddy current nature. It should be noted that, in [22], the prominent components of the stray load losses are generally computed as proportional to the squared stator current. Moreover, certain components of stray load losses are proportional to a power of the rotational speed, with the value of that power ranging from 1.5 to 2 [21]. For the purpose of this study, the stray load losses are recalculated as:

$$p_{sll} = i_{s1}^2 t_{par}^{0.9} \quad (43)$$

where  $t_{par}$  is the relative value of the parabolic load torque according to (9).

## IV. MATHEMATICAL DESCRIPTION OF THE COEFFICIENT OF VOLTAGE ENERGY EFFICIENCY

### A. PRELIMINARY REMARKS

Machine and load parameters exert a significant influence on the power losses occurring in an induction motor under power quality disturbances. In order to depict the problem, Figs. 4 to 7 present the relative power losses  $p_{tot}$  (relative to the value under nominal supply and a given load torque  $P_{ref}$ ) for various supply conditions and load parameters, for two induction motors of different properties: a TSg 100L-4B with a rated power of 3 kW, and a Sg 132-S4 with a rated power of 5.5 kW. The former has a comparatively strongly saturated magnetic circuit [14] and is particularly susceptible to overvoltage [14], whereas the latter is comparatively weakly saturated [14]. The relative power losses  $p_{tot}$  are computed using the method presented in Section III, for two values of the reference load torque, namely  $T_{ref} = 60\%$  of  $T_{rat}$  and  $T_{ref} = 90\%$  of  $T_{rat}$ , and two torque-speed characteristics of the load, namely a constant torque (TC) and a parabolic load torque (PL). For the latter, the load torque is assumed to be equal to  $T_{ref}$  under nominal supply, while for the former, the supply conditions are recalculated using (9).

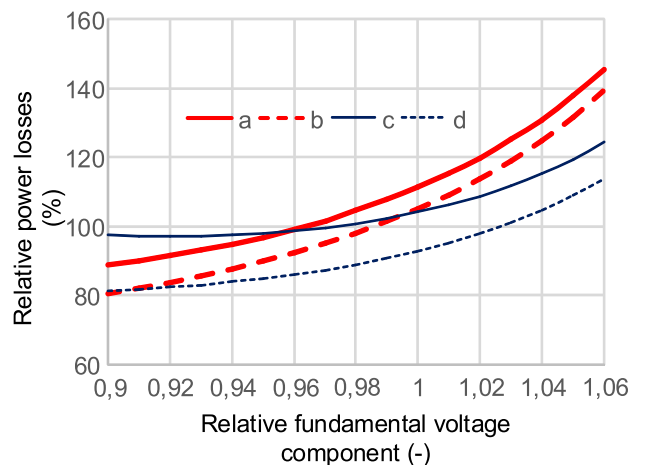


**FIGURE 4.** Relative power losses  $p_{tot}$  versus relative value of fundamental voltage component  $u_1$  for induction cage machine TSg 100L-4B and supply voltage frequency of 95% of  $f_{rat}$ : a) reference load torque  $T_{ref} = 60\%$  of  $T_{rat}$ , TC; b) reference load torque  $T_{ref} = 60\%$  of  $T_{rat}$ , PL; c) reference load torque  $T_{ref} = 90\%$  of  $T_{rat}$ , TC; d) reference load torque  $T_{ref} = 90\%$  of  $T_{rat}$ , PL.

The relative power losses  $p_{tot}$  for the frequency of the supply voltage  $f = 95\%$  of  $f_{rat}$  versus the supply voltage within the range of 90% to 106% of  $U_{rat}$  are presented in Figs. 4 and 5. For the induction motor TSg 100L-4B (Fig. 4) and the reference torque  $T_{ref} = 60\%$  of  $T_{rat}$ , the power losses  $p_{tot}$  reach values as high as 145.7% of  $P_{ref}$  and 139.7% of  $P_{ref}$ , for TC and PL respectively. For the reference torque  $T_{ref} = 90\%$  of  $T_{rat}$ , the power losses  $p_{tot}$  reach a maximum of 124.6% of  $P_{ref}$ . For the other induction motor, the Sg 132-S4 (Fig. 5), the power losses  $p_{tot}$  do not exceed approximately 106% of  $P_{ref}$  for TC, while for PL, they remain below  $P_{ref}$ .

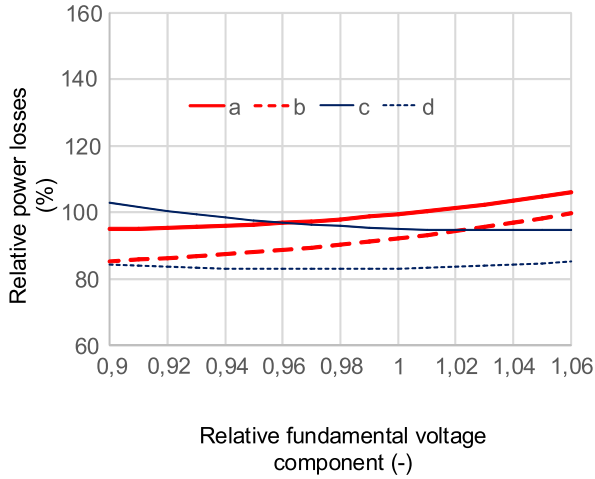


**FIGURE 5.** Relative power losses  $p_{tot}$  versus relative value of fundamental voltage component  $u_1$  for induction cage machine Sg 132-S4 and supply voltage frequency of 95% of  $f_{rat}$ : a) reference load torque  $T_{ref} = 60\%$  of  $T_{rat}$ , TC; b) reference load torque  $T_{ref} = 60\%$  of  $T_{rat}$ , PL; c) reference load torque  $T_{ref} = 90\%$  of  $T_{rat}$ , TC; d) reference load torque  $T_{ref} = 90\%$  of  $T_{rat}$ , PL.

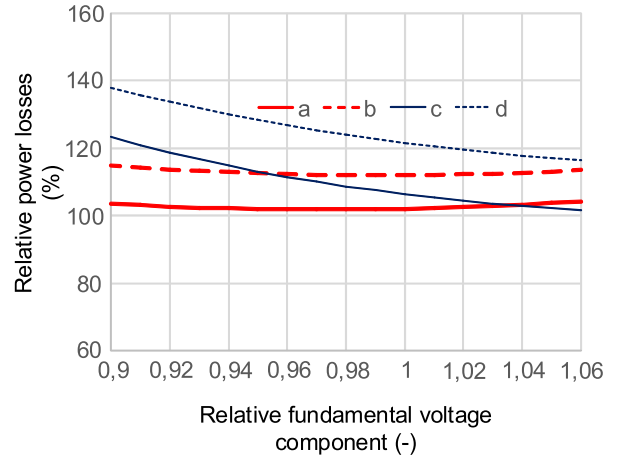


**FIGURE 7.** Relative power losses  $p_{tot}$  versus relative value of fundamental voltage component  $u_1$  for induction cage machine Sg 132-S4 and supply voltage frequency of 105% of  $f_{rat}$ : a) reference load torque  $T_{ref} = 60\%$  of  $T_{rat}$ , TC; b) reference load torque  $T_{ref} = 60\%$  of  $T_{rat}$ , PL; c) reference load torque  $T_{ref} = 90\%$  of  $T_{rat}$ , TC; d) reference load torque  $T_{ref} = 90\%$  of  $T_{rat}$ , PL.

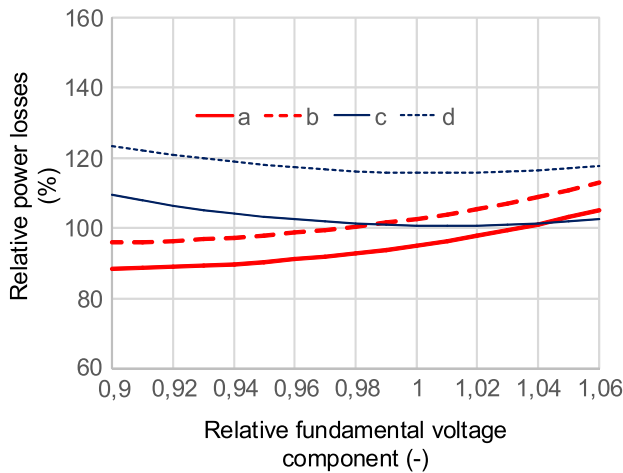


**FIGURE 6.** Relative power losses  $p_{tot}$  versus relative value of fundamental voltage component  $u_1$  for induction cage machine TSg 100L-4B and supply voltage frequency of 105% of  $f_{rat}$ : a) reference load torque  $T_{ref} = 60\%$  of  $T_{rat}$ , TC; b) reference load torque  $T_{ref} = 60\%$  of  $T_{rat}$ , PL; c) reference load torque  $T_{ref} = 90\%$  of  $T_{rat}$ , TC; d) reference load torque  $T_{ref} = 90\%$  of  $T_{rat}$ , PL.

The power losses  $p_{tot}$  versus voltage for the frequency  $f = 105\%$  of  $f_{rat}$  are presented in Figs. 6 and 7. For the induction motor TSg 100L-4B (Fig. 6), the power losses  $p_{tot}$  reach up to 123.7% of  $P_{ref}$  and 109.5% of  $P_{ref}$ , for PL and TC, respectively. It is worth noting that, for  $T_{ref} = 60\%$  of  $T_{rat}$ , the characteristics for  $p_{tot} = f(u)$  increase, while they decrease for  $T_{ref} = 90\%$  of  $T_{rat}$ . Further, for the induction motor Sg 132-S4 (Fig. 7) and  $T_{ref} = 90\%$  of  $T_{rat}$ , the relative power losses  $p_{tot}$  reach a maximum of 137.7% of  $P_{ref}$  and 123.5% of  $P_{ref}$ , for PL and TC, respectively. For  $T_{ref} = 60\%$  of  $T_{rat}$ , the power losses  $p_{tot}$  do not exceed 113.5% of  $P_{ref}$ .

The above examples demonstrate that the effects of the power quality disturbances on the power losses in an

induction cage motor depend substantially on the machine parameters and the load parameters. The same power quality disturbances may result in a significant increase in the power losses in one motor, whereas a reduction may even occur in another motor, in comparison to the nominal supply. Therefore, various combinations of load and machine parameters are considered for the calculation of the *coefficient of voltage energy efficiency*, and the actual value of the coefficient corresponds to the *worst* of the considered cases (for example, an induction motor with a weakly saturated magnetic circuit working under a parabolic load). An excessive value of  $p_{tot}$  (see the definition of the *coefficient of voltage energy efficiency* in Section III) will result in a significant increase in the level of power losses in certain installed motors, caused by power quality disturbances. The analysis of the load parameters and the induction motor parameters required for the determination of the coefficient is presented in the following subsections.

### B. LOAD PARAMETERS

In land power systems, the average load factor of the induction motors,  $L_f$  (the ratio of the power on the shaft in real working conditions to the rated power), is close to 60% (based on [23]). It should be noted that the load factors of different machines are highly diversified. Various surveys [23], [24] have revealed that there are motors working with a very small load factor, such as 3% to 16%, as well as motors working with a load factor close to the rated value, and in some cases even above this value. A similar situation occurs in ship power systems. In these systems, motors working with various load factors can be expected, including significantly oversized machines [25], [26].

According to [23], the main reason for oversizing is poor motor system design and a gross overestimation of the power on the shaft required by the load. It should be noted that



significant oversizing of induction motors is considered to be detrimental. Firstly, the machine efficiency has a strong dependence on the load factor. For a load factor  $L_f$  close to zero, the efficiency may be many times less than the maximal motor efficiency. Secondly, oversized induction motors consume excessive reactive power. In certain cases, the generators on a ship may even be overloaded. Such a case was analysed in [26]. During seagoing, the active power produced by the generator was approximately 45% of its rated power, but the generator was overloaded by the reactive power, owing to oversized induction motors [26]. As the operation of motors working with a load much less than the rated value is disadvantageous, it is recommended that significantly oversized motors should be replaced with ones of lower power [27].

Taking the above considerations into account, significantly oversized induction motors are not considered in the elaboration of the *coefficient of voltage energy efficiency*. For the purpose of this study, two values of the reference torque are assumed:  $T_{ref} = 60\%$  of  $T_{rat}$  and  $T_{ref} = 90\%$  of  $T_{rat}$ . Further, loads with two torque-speed characteristics are considered: constant torque loads and parabolic torque loads.

### C. MAGNETIC CIRCUIT PARAMETERS

According to the authors' experience regarding the operation of induction cage motors under power quality disturbances (for example, [7], [14]), frequency and voltage deviations are the power quality disturbances that cause the highest increase in the power losses. The following machines are particularly sensitive to these disturbances [7]:

- machines with a strongly saturated magnetic circuit and a comparatively high value of the magnetising current, working under a comparatively low load; and
- machines with a weakly saturated magnetic circuit and a comparatively low value of the magnetising current, working under a comparatively high load.

Two parameters discussed in Section III can be used to describe the properties of such machines: the coefficient  $k_{im}$  and the normalised magnetising current (referred to as the stator current under reference working conditions)  $i_{mref}$ . For the purpose of determining the *coefficient of voltage energy efficiency*, the coefficient  $k_{im}$  is assumed to take the values 1 and 3, for machines with weakly and strongly saturated magnetic circuits, respectively (based on [7]). Further, based on the authors' experience and [7], the corresponding values for the normalised magnetising current are assumed to be  $i_{mnom} = 0.35$  and  $i_{mnom} = 0.5$ , respectively. It should be noted that, for the partial loads  $T_{ref} = 60\%$  of  $T_{rat}$  and  $T_{ref} = 90\%$  of  $T_{rat}$ , the value of  $i_{mnom}$  is recalculated as  $i_{mref}$  (see Section II), using the method presented in Section III.

Additional analysis of the effects of the load parameters and the machine parameters on the power losses under power quality disturbances may be carried out. For the purpose of this study, the following cases are considered:

- a) machines with a strongly saturated magnetic circuit and a comparatively high value of the magnetising current, working under constant torque loads with  $T_{ref} = 60\%$  of  $T_{rat}$ ;
- b) machines with a strongly saturated magnetic circuit and a comparatively high value of the magnetising current, working under parabolic torque loads with  $T_{ref} = 60\%$  of  $T_{rat}$ ;
- c) machines with a weakly saturated magnetic circuit and a comparatively low value of the magnetising current, working under constant torque loads with  $T_{ref} = 90\%$  of  $T_{rat}$ ; and
- d) machines with a weakly saturated magnetic circuit and a comparatively low value of the magnetising current, working under parabolic torque loads with  $T_{ref} = 90\%$  of  $T_{rat}$ .

As mentioned previously, the actual values of the coefficient correspond to the *worst* of the considered cases; these values indicate that the power losses in certain installed induction motors increase significantly as a result of the power quality disturbances.

### D. EFFICIENCY AND FRACTIONS OF POWER LOSSES

According to various international and national regulations, new induction motors are generally required to exhibit an efficiency class [28] of at least IE3. Nevertheless, motors with efficiency classes of IE4 are available on the market and numerous motors of lower efficiency classes remain in operation. Furthermore, the efficiencies of many induction motors of the IE3 class correspond to the threshold value of this class. Therefore, this threshold value is assumed for the purpose of determining the *coefficient of voltage energy efficiency*. It should be noted that the exact value of this threshold is significantly affected by the machine rated power. According to [28], for 50 Hz, four-pole motors, the threshold values are 95.2% and 91.4% for motors with rated powers of 90 kW and 11 kW, respectively.

The distribution of power losses assumed in this study is represented in Fig. 8 [29]. This distribution represents the typical contributions of the various components of the power losses in four-pole induction motors, versus the rated power. For the partial load, the contribution of the power losses in the stator windings is recalculated as follows:

$$w_{sw} = \frac{w_{sw\_nom} p_{sw}}{p_{tot}} \quad (44)$$

where  $w_{sw}$  denotes the contributions of the power losses in the stator windings to the total power losses under the reference working conditions (that is, for the nominal supply and  $T_{ref} = 60\%$  of  $T_{rat}$  or  $T_{ref} = 90\%$  of  $T_{rat}$ );  $w_{sw\_nom}$  denotes the contributions of the power losses in the stator windings to the total power losses, under nominal working conditions; and  $p_{sw}$  and  $p_{tot}$  are the relative power losses in the stator windings and the total power losses, respectively, under the reference working conditions, computed using the method presented in Section III.

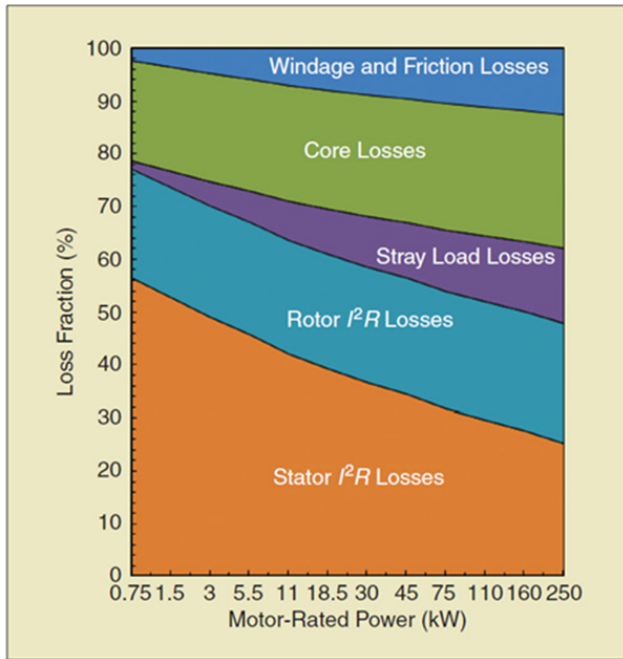


FIGURE 8. Typical fractions of power losses in four-pole induction cage motors [29].

The contributions of the components of the other power losses are recalculated in an analogous manner.

**E. SLIP AND PARAMETERS OF THE EQUIVALENT CIRCUIT**

The parameters of the equivalent circuit have a significant effect on the sensitivity of an induction motor to power quality disturbances.

Under voltage unbalance and voltage waveform distortions, the negative-sequence current component and the current harmonics are mainly suppressed by the leakage reactances. In this study, a comparatively small relative short-circuit reactance is assumed, equal to  $x_{sc} = 0.12$  (with reference to the nominal working conditions). The value  $x_{sc} = 0.12$  corresponds to a starting current of approximately 700% to 800% of the rated current (its detailed value depends on the resistance of the windings and the shape of the rotor bars). It should be noted that similar values for the starting current are often found for induction motors of the premium efficiency IE3 class (based on the analysis of catalogues of induction motors and [30]). Furthermore, the stator and rotor leakage reactances are assumed to have the same value, which is equal to half of the short-circuit reactance. This simplification is often applied during the analysis of induction machines.

The resistances existing in the equivalent circuit can be assessed based on a simplified analysis of each component of the power losses. The power losses in the stator windings under nominal working conditions are obtained as follows:

$$\Delta P_{sw\_nom} = w_{sw\_nom} S_{nom} p_{f\_nom} (1 - \eta_{nom}) \quad (45)$$

where  $S_{nom}$  is the apparent input power under nominal working conditions;  $p_{f\_nom}$  is the power factor under nominal working conditions; and  $\eta_{nom}$  is the efficiency under nominal working conditions.

As the relative stator current  $i_{s\_nom} = 1$  under nominal working conditions, the relative resistance of the stator windings ( $r_{s\_nom}$ ), understood as

$$r_{s\_nom} = \frac{R_s I_{s\_nom}}{U_{Nph}} \quad (46)$$

can be expressed as:

$$r_{s\_nom} = w_{sw\_nom} p_{f\_nom} (1 - \eta_{nom}) \quad (47)$$

The value of the power factor  $p_{f\_nom}$  can be determined by means of iterative calculations using the proposed method.

The power losses due to friction and windage, as well as several components of the stray load losses, are covered by the mechanical power produced by the rotor. However, for the purpose of a simplified analysis of the induction motor, the power transferred from the stator to the rotor by the rotating magnetic field ( $P_{mag}$ ) can be approximated as follows:

$$P_{mag} = P_{in} \left( 1 - \frac{\Delta P_{tot} - \Delta P_{rw}}{\Delta P_{tot}} \right) \quad (48)$$

where  $P_{in}$  is the input machine power;  $\Delta P_{tot}$  represents the total power losses (in Watts); and  $\Delta P_{rw}$  denotes the power losses in the rotor windings (in Watts).

Taking into account that, for nominal working conditions, the contribution of the power losses in the rotor windings is defined as:

$$w_{rw\_nom} = \frac{\Delta P_{rw\_nom}}{\Delta P_{tot\_nom}} \quad (49)$$

and that the power losses in the rotor windings are equal to the following, for the assumed simplifications:

$$\Delta P_{rw} = s_{nom} P_{mag} \quad (50)$$

then, it follows that:

$$P_{in} [1 - (1 - \eta_{nom}) (1 - w_{rw\_nom})] (1 - s_{nom}) = \eta_{nom} P_{in} \quad (51)$$

and the slip under nominal working conditions can be expressed as:

$$s_{nom} = 1 - \frac{\eta_{nom}}{1 - (1 - \eta_{nom}) (1 - w_{rw\_nom})} \quad (52)$$

For the purpose of a simplified analysis, it can be assumed that the iron current  $I_{Fe}$  covers both the actual iron losses and the mechanical losses [21]. Under nominal working conditions, the sum of these losses amounts to:

$$\begin{aligned} \Delta P_{Fe} + \Delta P_m &= 3U_{Nph} I_N p_{f\_nom} (1 - \eta_{nom}) (w_{Fe\_nom} + w_{m\_nom}) \\ &= 3EI_{Fe} \end{aligned} \quad (53)$$

where  $\Delta P_{Fe}$  and  $\Delta P_m$  are the iron losses and mechanical power losses (in Watts), respectively;  $I_N$  is the nominal current;  $w_{Fe\_nom}$  and  $w_{m\_nom}$  are the contributions of the iron

losses and the mechanical losses to the total losses, respectively; and  $E$  is the electromotive force.

As the relative stator current  $i_{s\_nom} = 1$  under nominal working conditions, the value of the electromotive force (relative to the supply voltage) is represented by the following approximation:

$$e_{nom} \approx 1 - r_s p_{f\_nom} - x_s \sqrt{1 - p_{f\_nom}^2} \quad (54)$$

As a result, the relative iron current under nominal working conditions,  $i_{Fe\_nom}$ , may be estimated as:

$$i_{Fe\_nom} = p_{f\_nom} (1 - \eta_{nom}) \frac{W_{Fe\_nom} + W_{m\_nom}}{e_{nom}} \quad (55)$$

The relative value of the magnetising current  $i_{m\_nom}$  was assumed in subsection IV C. The currents  $i_{Fe\_nom}$  and  $i_{m\_nom}$  can be recalculated by using the iron resistance and the magnetising reactance. The resistance of the rotor windings and the ratio of the rotor current to the nominal current can be determined by means of iterative calculations with the equivalent circuit. Subsequently, all of the currents, resistances, and reactances may be recalculated under the reference working conditions (that is, for the nominal supply and  $T_{ref} = 60\%$  of  $T_{rat}$  or  $T_{ref} = 90\%$  of  $T_{rat}$ ), using the method presented in Section III and the expressions analogous to (56):

$$r_s = r_{s\_nom} \frac{i_{s\_ref}}{i_{s\_nom}} \quad (56)$$

### F. MACHINE RATED POWER

As mentioned previously, the voltage and frequency deviations are those power quality disturbances that cause the highest increase in the power losses in induction motors. This increase depends on the machine power, among other factors. For the voltage and frequency deviations permitted in ship power systems (see Section II), and machines with a rated power of 90 kW and parameters estimated with the methods presented here, the relative power losses  $p_{tot}$  reach values as high as 133.6% of  $P_{ref}$  (for  $T_{ref} = 60\%$  of  $T_{rat}$ ). For machines with a rated power of 11 kW, the relative power losses  $p_{tot}$  reach values as high as 141.4% of  $P_{ref}$  (for  $T_{ref} = 60\%$  of  $T_{rat}$ ).

The above example demonstrates that voltage and frequency deviations may cause considerably greater percentage increases in power losses in machines with low power than in machines with high power. For this reason, a motor power of approximately 10 kW is assumed for the purposes of calculating the *coefficient of voltage energy efficiency*.

### G. AMBIENT TEMPERATURE AND TEMPERATURE IN THE WINDINGS

The increase in the temperature of the windings under nominal working conditions,  $\Delta\vartheta_{nom}$ , affects the sensitivity of the induction motors to power quality disturbances. A higher increase in  $\Delta\vartheta_{nom}$  produces more significant additional machine heating under power quality disturbances. The additional heating causes an increment in the resistance of

the windings and, consequently, an additional increase in the ohmic losses, as explained in Section III. For the purpose of this study, the increase in the temperature of the windings is assumed to be  $\Delta\vartheta_{nom} = 80$  K, which roughly corresponds to the maximal permissible level for insulation of class B. However, for premium-efficiency machines, the increase in the temperature of the windings may have a considerably lower value [30]. The increase of  $\Delta\vartheta_{nom} = 80$  K is recalculated for reference working conditions (nominal supply and a reference load torque  $T_{ref} = 60\%$  of  $T_{rat}$  or  $T_{ref} = 90\%$  of  $T_{rat}$ ), based on the method presented in Section II, and an assumed ambient temperature of  $\vartheta_0 = 40^\circ\text{C}$ . Finally, for the cases considered in subsection IV C, the reference increase in the temperature of the windings is assumed to be  $\Delta\vartheta_{ref} = 50$  K and  $\Delta\vartheta_{ref} = 70$  K, for the reference load torques of  $T_{ref} = 60\%$  of  $T_{rat}$  and  $T_{ref} = 90\%$  of  $T_{rat}$ , respectively.

### H. APPROXIMATION OF POWER LOSSES – COEFFICIENT OF VOLTAGE ENERGY EFFICIENCY

The mathematical description of the power losses, presented in Section III, is not convenient for implementation in power quality analysers, standards, rules, and everyday practice. Consequently, the elaboration of the *coefficient of voltage energy efficiency* ( $c_{vee}$ ) requires an appropriate approximation of the power losses with simplified expressions that are easy to calculate. For the sake of simplicity, the applied approximation is based on the summation of the power losses due to each respective disturbance of the power quality (although, according to the authors' experience, there exists a small synergy):

$$p_{tot} = c_{vee} = p_{fund} + p_{har} + p_{unbal} \quad (57)$$

where  $p_{fund}$  represents the relative power losses due to the fundamental voltage harmonic,  $p_{har}$  indicates the relative power losses caused by the voltage harmonics, and  $p_{unbal}$  represents the relative power losses caused by the voltage unbalance:

$$p_{fund} = \max(p_{fund1}, p_{fund2}) \quad (58)$$

$$p_{fund1} = f_*^{2.9} \left( c_1 u_*^{-3} \Delta u_*^3 + c_2 u_*^{-3} + c_3 u_*^{-1} \right) \quad (59)$$

$$p_{fund2} = f_*^{2.9} \left( c_4 \Delta u_*^2 + u_*^{0.7} \right) \quad \text{for } \Delta u_* \geq 0 \quad (60a)$$

$$p_{fund2} = f_*^{2.9} \left( -c_4 \Delta u_*^2 + u_*^{0.7} \right) \quad \text{for } \Delta u_* < 0 \quad (60b)$$

$$f_* = f \quad \text{for } f > 1 \quad (61a)$$

$$f_* = 1 \quad \text{for } f \leq 1 \quad (61b)$$

$$u_* = f^{1.45} u^{-1} \quad \text{for } f > 1 \quad (62a)$$

$$u_* = f u^{-1} \quad \text{for } f \leq 1 \quad (62b)$$

$$\Delta u_* = u_* - 1 \quad (63)$$

$$p_{har} = \sum_{h=2,5,11,\dots}^{hmax} u_h^2 \left( c_{h1} f_h^{-1.2} + c_{h2} f_h^{-1.7} \right) + \sum_{h=4,7,13,\dots}^{hmax} u_h^2 \left( c_{h3} f_h^{-1.2} + c_{h4} f_h^{-1.7} \right) \quad (64)$$

$$p_{unbal} = c_- u_-^2 \quad (65)$$

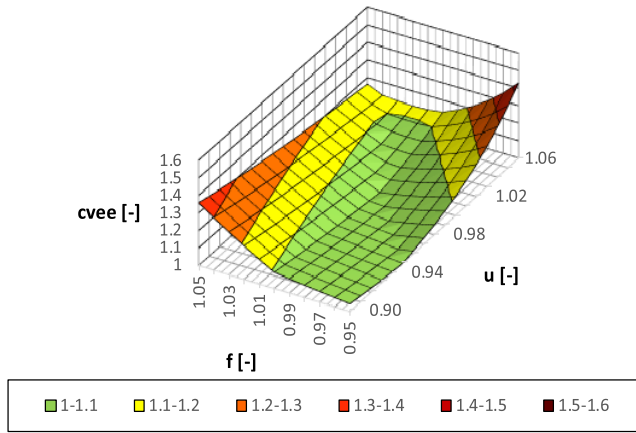


FIGURE 9. Coefficient of voltage energy efficiency  $c_{vee}$  versus relative frequency and voltage, related to its rated values.

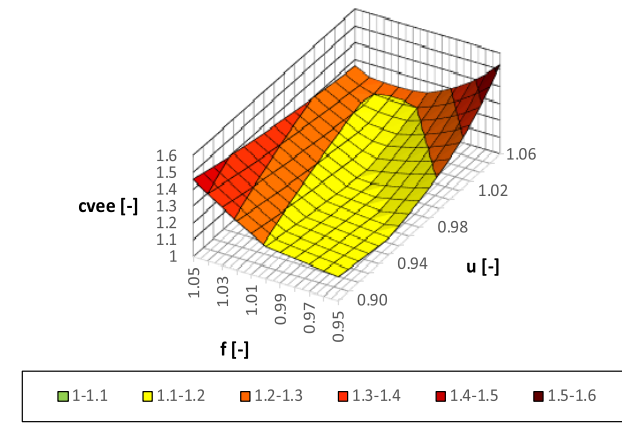


FIGURE 10. Coefficient of voltage energy efficiency  $c_{vee}$  versus relative frequency and voltage (related to its rated values), for 2% voltage unbalance and the following voltage harmonics:  $U_5 = 5\%$  of  $U_{rat}$ ,  $U_7 = 4\%$  of  $U_{rat}$ ,  $U_{11} = 3.5\%$  of  $U_{rat}$  and  $U_{13} = 3.5\%$  of  $U_{rat}$ .

where  $c_1 = -150$ ,  $c_2 = 0.3$ ,  $c_3 = 0.7$ ,  $c_4 = 1.3$ ,  $c_{h1} = 7000$ ,  $c_{h2} = 50000$ ,  $c_{h3} = 7000$ ,  $c_{h4} = 15000$ , and  $c_- = 125$ .

All voltage parameters in the above expressions are per unit, relative to the rated voltage and frequency. For example, for the negative-sequence voltage equal to 3% of  $U_{rat}$ ,  $u_- = 0.03$  and  $p_{unbal}$  calculated with (65) has the value 0.1125. The above approximation is only valid for machines with the assumed parameters. It should be noted that  $p_{fund1}$  and  $p_{fund2}$  correspond to the machines specified in subsection IV C, in points *a*, *b* and *c*, *d*, respectively. The expression  $f_*^{2.9}$  models an increase in the power losses owing to the speed variation under a parabolic load torque. The first summand in (64) corresponds to the negative-sequence voltage harmonics, whereas the second summand corresponds to the positive-sequence voltage harmonics (harmonics of orders that are integer multiples of 3 are omitted).

The expressions in (57) to (65) constitute a mathematical description of the coefficient of voltage energy efficiency. The variation of this coefficient is mapped in Fig. 9, for a range of voltage and frequency deviations. In Fig. 10, the variation of

the coefficient is mapped for a range of voltage and frequency deviations combined with a 2% voltage unbalance ( $U_- = 2\%$  of  $U_{rat}$ ) and voltage waveform distortions. The values of the voltage harmonics are:  $U_5 = 5\%$  of  $U_{rat}$ ,  $U_7 = 4\%$  of  $U_{rat}$ ,  $U_{11} = 3.5\%$  of  $U_{rat}$ , and  $U_{13} = 3.5\%$  of  $U_{rat}$ . These values are based on a voltage waveform recorded in a real ship power system. For the mapping of the coefficient for a range of voltage and frequency deviations harmonics (Fig. 10), the maximal value increases to 1.54.

The coefficient of voltage energy efficiency is experimentally verified in the following section.

### V. EXPERIMENTAL VERIFICATION OF THE COEFFICIENT OF VOLTAGE ENERGY EFFICIENCY

The model of power losses presented in Section III is applied for the elaboration of the coefficient of voltage energy efficiency. To verify the coefficient, the power losses calculated using this model ( $P_{calc}$ ) are compared with their value determined from measurements ( $P_{meas}$ ). Furthermore, the power losses  $P_{meas}$  are collated with the values of the coefficient  $c_{vee}$ .

The power losses model is validated for four induction machines, denoted by *motor 1*, *motor 2*, *motor 3*, and *motor 4*, respectively, with different properties. *Motor 1* has a comparatively strongly saturated magnetic circuit [14] and is particularly sensitive to overvoltage. In contrast, *motor 2* and *motor 4* have comparatively weakly saturated magnetic circuits [14] and are particularly susceptible to undervoltage. Further, the magnetic circuit of *motor 3* is medium saturated. This motor is sensitive to both overvoltage and undervoltage, but its increase in power losses is less than those in *motor 1*, *motor 2*, and *motor 4*. It should be noted that *motor 1* and *motor 2* are of efficiency class EF1, whereas *motor 3* and *motor 4* are of class IE3. The basic parameters of the machines are listed in Table 1. It is also worth mentioning that the stator and rotor of *motor 2* are equipped with thermocouples, the locations of which are presented in [14]. In practice, some components of the power losses can be determined from the results of machine heating tests and analysis using a thermal equivalent circuit, presented and described in [14].

TABLE 1. Basic parameters of the Investigated motors.

Motor	Motor 1	Motor 2	Motor 3	Motor 4
type	TSg100 L-4B	Sg132S-4	3SIE100 L4B	1LE100 3-1BB22-2AA4
Rated power (kW)		5.5	3	4
Rated frequency (Hz)	50	50	50	50
Rated voltage (V)	380	380	400	400
Rated current (A)	6.9	11.4	6.3	7.9
Rated power factor (-)	0.81	0.85	0.79	0.82
Rated rotational speed	1420	1445	1465	1460
No-load current (% of $I_{rat}$ )	60	40	60	50

The investigated induction motors are loaded with DC generators feeding resistor banks. It should be noted that, for power quality disturbances causing an increase in the rotational speed (for example, due to an increase in the frequency), the load torque value is increased in proportion to the squared value of the speed. The programmable AC power source Chroma 6590-3 with a rated power of 9 kVA is employed to supply the motors. The power source enables the precise setting of various power quality disturbances, namely voltage and frequency deviations, voltage unbalance, and programmable voltage harmonics. The unbalance degree is measured using a power quality estimator–analyser, which was developed by one of the co-authors for commercial purposes and is certified by the Polish Register of Shipping. Furthermore, a computer-based power quality analyser is used. An example configuration of the measurement setup is presented in Fig. 11.

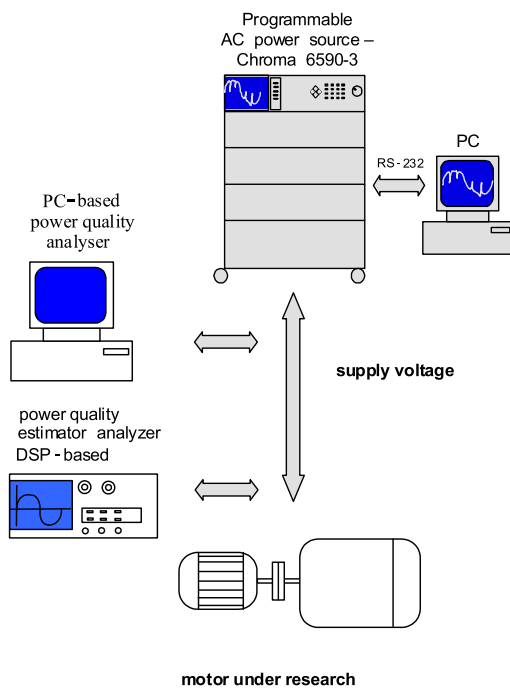


FIGURE 11. Example configuration of measurement setup.

For the sinusoidal voltage, balanced supply voltage power losses in the rotor windings are identified on the grounds of measurements of the rotational speed and output power. Moreover, for the sinusoidal voltage, balanced voltage power losses in iron, mechanical losses, and stray load losses are recalculated from their values for the nominal supply based on measurements of the current, voltage, rotational speed, winding resistance, and power factor (used for calculating the stator winding electromotive force and iron losses). It should be noted that, according to the provisions of the standard *IEC/EN 60034-2-1 Rotating electrical machines — Part 2-1 Standard methods for determining losses and efficiency from tests (excluding machines for traction vehicles)* [13], the separation of the power losses in iron and mechanical losses is

based on the assumption that the power losses in iron are proportional to the squared value of the supply voltage. Furthermore, the standard [13] recommends the recalculation of stray load losses for each load point. For all supply conditions, the power losses in the stator windings are determined from measurements of the RMS current value and the resistance (or temperature) of the windings after long-lasting work. Several power losses are identified for the voltage unbalance and voltage harmonics (for example, the power losses in a rotor), on the grounds of thermal tests and thermal analysis.

A comparison of the power losses  $P_{meas}$  and  $P_{calc}$  is presented in Table 2, for various power quality disturbances and two values of the reference load torque (that is, for the reference test for the nominal supply): 60% of  $T_{rat}$  and 90% of  $T_{rat}$ . As mentioned previously, for given power quality disturbances, the *coefficient of voltage energy efficiency* corresponds to the *worst* of the various sets of machine and load parameters (see subsection IV C for a detailed explanation). Therefore, the combinations of power quality disturbances, motors, and reference torques resulting in a reduction or a comparatively low increase in the power losses are not included in Table 2. Further, for case 17 (with a 5th harmonic of value  $U_5 = 9.2\%$  of  $U_{rat}$ ; see Table 2), the approximate value of  $P_{meas}$  is presented for informative purposes only, because of the measurement uncertainty. For the voltage waveform distortions, the model is validated for a much higher voltage harmonic value: for the 5th voltage harmonic  $U_5 = 20\%$  of  $U_{rat}$ . The results of the appropriate thermal tests (used for the determination of  $P_{meas}$ ) are presented in Fig. 12. For the case under consideration, the power losses  $P_{meas} = 114\%$  of  $P_{ref}$  and  $P_{calc} = 111.2\%$  of  $P_{ref}$ .

The collation of the power losses  $P_{meas}$  and  $P_{calc}$  for diverse power quality disturbances demonstrates that the applied model of power losses is characterised by acceptable accuracy for the purpose of this study, although significant discrepancies occur in some cases. For example, for case 7 (see Table 2),  $P_{meas} = 145\%$  of  $P_{ref}$  and  $P_{calc} = 137.7\%$  of  $P_{ref}$ . For case 9,  $P_{meas} = 133\%$  of  $P_{ref}$  and  $P_{calc} = 127.9\%$  of  $P_{ref}$ .

Table 2 also presents the results of investigations concerning an increase in the input power and a decrease in the efficiency under power quality disturbances, for motors 1 to 4. The values of the coefficient  $c_{vee}$  corresponding to each case specified in Table 2 are provided in Table 3. For each of the considered cases, the value of the power losses  $P_{meas}$  is comparable to the coefficient  $c_{vee}$  for at least one motor. The only exceptions are the voltage harmonics and voltage waveform distortions (cases 16 and case 17). In these cases, the power losses conforming to the value of  $c_{vee}$  are significantly greater than  $P_{meas}$ . This is due to the fact that an increase in power losses caused by voltage unbalance and voltage waveform distortions is highly sensitive to the machine parameters, particularly to the value of the short-circuit reactance. In practice, the increase in the power losses can be considered as approximately inversely proportional to the squared short-circuit reactance value. For *motor 2*, the

**TABLE 2.** Power losses determined from measurements ( $P_{meas}$ ), calculated power losses ( $P_{calc}$ ), increases in input power and decreases in efficiency, for the investigated motors and various power quality disturbances.

Case	Motor	Power quality disturbances	Reference load torque [% of $T_{rat}$ ]	Power losses $P_{meas}$ [% of $P_{ref}$ ]	Power losses $P_{calc}$ [% of $P_{ref}$ ]	Increase in input power [%]	Decrease in efficiency [%]
1	Motor 1	$f=95\%$ of $f_{rat}$ , $U=106\%$ of $U_{rat}$	60%	143%	145.7%	5%	6.5%
2	Motor 3	$f=95\%$ of $f_{rat}$ , $U=106\%$ of $U_{rat}$	60%	125%	126.4%	-1.5%	3.5%
3	Motor 1	$f=95\%$ of $f_{rat}$	60%	111%	111.3%	-1.5%	2.5%
4	Motor 3	$f=95\%$ of $f_{rat}$	60%	106.5%	105.5%	-4.5%	1.5%
5	Motor 1	$U=106\%$ of $U_{rat}$	60%	118%	118.1%	4.5%	2.5%
6	Motor 3	$U=106\%$ of $U_{rat}$	60%	112%	113%	1.5%	1.5%
7	Motor 2	$f=105\%$ of $f_{rat}$ , $U=90\%$ of $U_{rat}$	90%	145%	137.7	15%	3.5%
8	Motor 3	$f=105\%$ of $f_{rat}$ , $U=90\%$ of $U_{rat}$	90%	119%	118.1%	13%	0.5%
9	Motor 4	$f=105\%$ of $f_{rat}$ , $U=90\%$ of $U_{rat}$	90%	133%	127.9%	14%	2%
10	Motor 2	$f=105\%$ of $f_{rat}$	90%	125%	121.6%	15.5%	1%
11	Motor 3	$f=105\%$ of $f_{rat}$	90%	113%	113.2%	14%	<0.5%
12	Motor 4	$f=105\%$ of $f_{rat}$	90%	119%	117.5%	15.5%	0.5%
13	Motor 2	$U=90\%$ of $U_{rat}$	90%	113%	112.3%	0.5%	1.5%
14	Motor 3	$U=90\%$ of $U_{rat}$	90%	101%	100.6%	0.5%	<0.5%
15	Motor 4	$U=90\%$ of $U_{rat}$	90%	107.5%	106.1%	1%	1%
16	Motor 2	$U_5=3\%$ of $U_{rat}$	60%	103.5%	103.6%	0.5%	0.5%
17	Motor 2	$U_5=9.2\%$ of $U_{rat}$	60%	(104.5%)	103.2%	<0.5%	0.5%

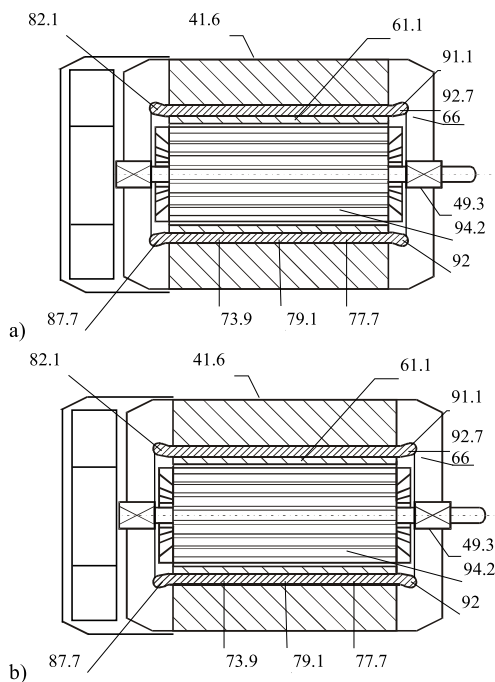


**FIGURE 12.** Distribution of measured temperature rise in motor 2 with rated load torque, and: a) the nominal supply and an ambient temperature  $\vartheta_0 = 24.9^\circ\text{C}$ ; b) a fundamental voltage component  $U_1 = U_{rat}$ , the 5th voltage harmonic  $U_5 = 20\%$  of  $U_{rat}$  and an ambient temperature  $\vartheta_0 = 24.6^\circ\text{C}$ .

short-circuit reactance is  $x_{sc} = 0.186$  (with reference to the nominal working conditions), while its value assumed for the coefficient elaboration is  $x_{sc} = 0.12$ .

The most significant increase in the input power, an increase of 15.5%, is observed for motor 2 and motor 4,

under a frequency of  $f = 105\%$  of  $f_{rat}$  (cases 10, 12). The most significant decrease in the efficiency, a decrease of 6.5%, occurs for motor 1, for a voltage frequency of  $f = 95\%$  of  $f_{rat}$  and a voltage value of  $U = 106\%$  of  $U_{rat}$  (case 1).

**TABLE 3.** Values of the coefficient of voltage energy efficiency  $c_{vee}$  and the temperature coefficient of power quality  $c_{pqs}$  for cases specified in Table 2.

Case	Power quality disturbances	$c_{vee}[-]$	$c_{pqs}[-]$
1-2	$f=95\%$ of $f_{rat}$ , $U=106\%$ of $U_{rat}$	1.43	1.30
3-4	$f=95\%$ of $f_{rat}$	1.108	1.045
5-6	$U=106\%$ of $U_{rat}$	1.132	1.083
7-9	$f=105\%$ of $f_{rat}$ , $U=90\%$ of $U_{rat}$	1.359	1.738
10-12	$f=105\%$ of $f_{rat}$	1.219	1.353
13-15	$U=90\%$ of $U_{rat}$	1.093	1.299
16	$u_5=9.2\%$ of $U_{rat}$	1.114	1.037
17	$u_5=3\%$ of $U_{rat}$	1.112	1.156

The highest increase in the power losses, an increase of 45%, appears for motor 2, for  $f = 105\%$  of  $f_{rat}$  and a voltage value of  $U = 90\%$  of  $U_{rat}$  (case 7). It should be noted that motor 4 is less sensitive to this voltage and frequency combination (case 9), probably owing to the higher value of the magnetising current (see Table 1 and considerations in subsection IV C). Consequently, for this voltage and frequency combination, the value of the  $c_{vee}$  coefficient (1.359—see Table 3) depends more powerfully on  $P_{meas}$  determined for motor 1 (see Table 3) than on  $P_{meas}$  determined for motor 4. Similarly, for cases 10-12 ( $f = 105\%$  of  $f_{rat}$ ), the value of the  $c_{vee}$  coefficient (1.219) depends

more powerfully on  $P_{meas}$  determined for *motor 1*. The above instances indicate that the  $c_{vee}$  coefficient should be used only for the assessment of the effect of power quality disturbances on a group of motors of various parameters (for example, all on-board grid-connected induction motors). Application of the coefficient for a particular motor only, may lead to inconsistent results because of differences between real machine parameters and the assumed ones (see Sections III, IV). However, the same method can be used for the calculation of the coefficient dedicated to a group of particular machines, if the machines with closed properties are used on-board of a particular ship, requiring modification of the parameters assumed for the coefficient elaboration (Sections III, IV).

Among the various power quality factors mentioned in Section II, only the *temperature coefficient of power quality* ( $c_{pqs}$ ) [7] can be used for the estimation of the effect of power quality disturbances on induction motors in a ship microgrid and is based on the machine models. Its value is proportional to the rise in the temperature of the windings (the difference between the temperature of the windings and the ambient temperature) of low-power induction motors under full load. For the negative-sequence voltage component  $U_- = 1\%$  of  $U_{rat}$  and  $U_- = 2\%$  of  $U_{rat}$ , the values of the coefficient are  $c_{pqs} = 1.044$  and  $c_{pqs} = 1.096$ , respectively. For the same voltage unbalance, the considered voltage energy efficiency coefficients are  $c_{vee} = 1.013$  and  $c_{vee} = 1.05$ , respectively. These values differ because the two coefficients serve different purposes. The *temperature coefficient of power quality* was intended for an assessment of the voltage quality on shortening life span of induction motors due to insulation thermal ageing. The differences between the above-mentioned results are due to the fact that the main reason for machine overheating under voltage unbalance is not related to an increase in total power losses, but to the unequal distribution of power losses among three-phase windings. Further comparisons of the values of these two coefficients are presented in Table 3 and show that the *temperature coefficient of power quality* is not an appropriate tool for the assessment of power losses in induction motors.

In summary, the applied model of power losses demonstrates that the *coefficient of voltage energy efficiency* ( $c_{vee}$ ) offers an assessment of acceptable accuracy. Although the parameters of motors of the IE3 efficiency class are assumed for the derivation of the coefficient  $c_{vee}$ , the coefficient can readily be employed for assessments of power losses in motors of other efficiency classes.

## VI. CONCLUSION

Power quality disturbances add significantly to the power losses occurring in induction motors. Moreover, the frequency and voltage deviations affect the rotational speeds of induction motors. Consequently, for motors working with parabolic torque loads, the power quality disturbances permitted in a ship power system [4] may even cause a 15% increase in the power on the shaft. Excessive power quality disturbances are often correlated with failures of on-board

equipment, and in extreme cases, these may even pose a threat to safety at sea.

Strict power quality monitoring in on-board microgrids may contribute to more energy-efficient ship operation, and improve safety while afloat. In this study, a dedicated tool for power quality monitoring has been proposed, namely the *coefficient of voltage energy efficiency* ( $c_{vee}$ ). This coefficient has a physical meaning and has been mathematically derived and experimentally verified. Its value is proportional to the power losses occurring in induction motors owing to power quality disturbances. A value of the  $c_{vee}$  coefficient close to unity indicates that the power quality disturbances do not cause considerable power losses in the induction motors. Further, an increased value indicates that the power quality disturbances cause significant power losses in at least some of the installed induction motors. The value of the *coefficient of voltage energy efficiency* can be determined from the indications of current power quality analysers, namely the frequency and voltage values, the harmonic content, and the degree of voltage unbalance. The mathematical description of the  $c_{vee}$  coefficient has been significantly simplified to enable easy implementation in standards, rules, and power quality analysers.

In subsequent papers, recommendations will be presented concerning the application of the new power quality coefficient. Furthermore, the results of power quality monitoring in ship microgrids, applying the  $c_{vee}$  coefficient, will be demonstrated for various operating conditions.

## REFERENCES

- [1] J. Mindykowski, "Power quality on ships: Today and tomorrow's challenges," in *Proc. Int. Conf. ExpoE Electr. Power Eng. (EPE)*, Iasi, Romania, Oct. 2014, pp. 16–18.
- [2] T. Tarasiuk, "Angular frequency variations at microgrids and its impact on measuring instruments performance," *IET Gener., Transmiss. Distrib.*, vol. 10, no. 13, pp. 3234–3240, Oct. 2016.
- [3] M. Mindykowski, "Contemporary challenges to power quality in ship systems-metrological perspective," in *Proc. 22nd IMEKO TC4 Int. Symp. 20th Int. Workshop ADC Modeling Test.*, Iasi, Romania, 2017, pp. 536–558.
- [4] *Electrical Installations in Ships—Part 101: Definitions and General Requirements*, IEC Standard 60092-101, 2018.
- [5] S. De and S. Debnath, "Optimal switching strategy of an SVC to improve the power quality in a distribution network," *IET Sci., Meas. Technol.*, vol. 13, no. 5, pp. 640–649, Jul. 2019.
- [6] S. X. Duarte and N. Kagan, "A power-quality index to assess the impact of voltage harmonic distortions and unbalance to three-phase induction motors," *IEEE Trans. Power Del.*, vol. 25, no. 3, pp. 1846–1854, Jul. 2010.
- [7] P. Gnaciński, "Effect of power quality on windings temperature of marine induction motors," *Energy Convers. Manage.*, vol. 50, no. 10, pp. 2463–2476, Oct. 2009.
- [8] D. P. Mishra and P. Ray, "Calculation of power quality factor of supply system using LabVIEW," in *Proc. Michael Faraday IET Int. Summit*, Sep. 2015, pp. 12–13.
- [9] M. Nagarjuna, P. C. Panda, and A. Sandeep, "Power quality factor improvement using shunt active power line conditioner," in *Proc. IEEE Int. Conf. Adv. Commun., Control Comput. Technol.*, May 2014, pp. 411–415.
- [10] H. Singh, M. Z. Abdullah, and A. Qutieshat, "Detection and classification of electrical supply voltage quality to electrical motors using the fuzzy-min-max neural network," in *Proc. IEEE Int. Electr. Mach. Drives Conf. (IEMDC)*, May 2011, pp. 961–965.

- [11] P. Sinha, S. Debnath, and S. K. Goswami, "A new wavelet and fuzzy based power quality index for distribution systems under stationary and nonstationary disturbances," in *Proc. Michael Faraday IET Int. Summit*, Kolkata, India, 2015, pp. 481–486, doi: 10.1049/cp.2015.1680.
- [12] J. Yang, S. Wang, C. Liu, R. Wang, J. Ma, K. Xu, and Q. Lu, "Power quality assessment based on combinatorial weight method of variance maximizing," *J. Phys., Conf. Ser.*, vol. 1087, Sep. 2018, Art. no. 052042.
- [13] *Rotating Electrical Machines—Part 2-1: Standard Methods for Determining Losses and Efficiency From Tests (Excluding Machines for Traction Vehicles)*, IEC/EN Standard 60034-2-1 2014.
- [14] P. Gnaciński, "Thermal loss of life and load-carrying capacity of marine induction motors," *Energy Convers. Manage.*, vol. 78, pp. 574–583, Feb. 2014.
- [15] F. G. G. de Buck, P. Giustelinck, and D. de Backer, "A simple but reliable loss model for inverter-supplied induction motors," *IEEE Trans. Ind. Appl.*, vol. IA-20, no. 1, pp. 190–202, Jan. 1984.
- [16] P. Gnaciński, "Prediction of windings temperature rise in induction motors supplied with distorted voltage," *Energy Convers. Manage.*, vol. 49, no. 4, pp. 707–717, Apr. 2008.
- [17] A. Shenkman and M. Chertkov, "Heat conditions of a three-phase induction motor by a one-phase supply," *IEE Proc. Electr. Power Appl.*, vol. 146, no. 4, pp. 361–367, Jul. 1999.
- [18] A. Boglietti, A. Cavagnino, M. Lazzari, and M. Pastorelli, "Predicting iron losses in soft magnetic materials with arbitrary voltage supply: An engineering approach," *IEEE Trans. Magn.*, vol. 39, no. 2, pp. 981–989, Mar. 2003.
- [19] C. Debruyne, J. Desmet, S. Derammelaere, and L. Vandevelde, "Derating factors for direct online induction machines when supplied with voltage harmonics: A critical view," in *Proc. IEEE Int. Electr. Mach. Drives Conf. (IEMDC)*, May 2011, pp. 1048–1052.
- [20] W. Latek, "Testing of electrical machines in industry," Wydawnictwo Naukowo-Techniczne, Warsaw, Poland, (in Polish), 1979.
- [21] B. Dubicki, "Electrical machines. Part III, induction motors," Państwowe Wydawnictwo Naukowe, Warsaw, Poland, (in Polish), Państwowe 1964.
- [22] D. W. Novotny and S. A. Nasar, "High frequency losses in induction motors," Univ. Wisconsin, Madison, WI, USA, NASA Contractor Rep. NAG3-940, Jun. 1991. [Online]. Available: <https://ntrs.nasa.gov/archive/nasa/casi.ntrs.nasa.gov/19910015251.pdf>
- [23] F. J. T. E. Ferreira and A. T. deAlmeida, "Method for in-field evaluation of the stator winding connection of three-phase induction motors to maximize efficiency and power factor," *IEEE Trans. Energy Convers.*, vol. 21, no. 2, pp. 370–379, Jun. 2006.
- [24] M. Thirugnanasambandam, M. Hasanuzzaman, R. Saidur, M. B. Ali, S. Rajakarunakaran, D. Devaraj, and N. A. Rahim, "Analysis of electrical motors load factors and energy savings in an indian cement industry," *Energy*, vol. 36, no. 7, pp. 4307–4314, Jul. 2011.
- [25] J. Prousalidis, G. Antonopoulos, P. Mouzakis, and E. Sofras, "On resolving reactive power problems in ship electrical energy systems," *J. Mar. Eng. Technol.*, vol. 14, no. 3, pp. 124–136, Sep. 2015.
- [26] J. M. Prousalidis, "The necessity of reactive power balance in ship electric energy systems," *J. Mar. Eng. Technol.*, vol. 10, no. 1, pp. 37–47, Jan. 2011.
- [27] IMO Train the Trainer (TTT). Course on Energy Efficient Ship Operation, Module 4—Ship Board Energy Management. International Maritime Organisation. [Online]. Available: <http://www.imo.org>
- [28] *Rotating Electrical Machines—Part 30-1: Efficiency Classes of Line Orated AC Motors*, IEC-EN Standard 60034-30-1, 2014.
- [29] A. T. De Almeida, F. J. T. E. T. E. Ferreira, and J. A. C. Fong, "Standards for efficiency of electric motors," *IEEE Ind. Appl. Mag.*, vol. 17, no. 1, pp. 12–19, Feb. 2011.
- [30] F. J. T. E. Ferreira, B. Leprettre, and A. T. de Almeida, "Comparison of protection requirements in IE2-, IE3-, and IE4-class motors," *IEEE Trans. Ind. Appl.*, vol. 52, no. 4, pp. 3603–3610, Jul. 2016.

**PIOTR GNACIŃSKI** (Member, IEEE) received the M.Sc., Ph.D., and D.Sc. degrees in electrical engineering from the Gdańsk University of Technology, Poland, in 1993, 2000, and 2011, respectively. Since 1993, he has been on the staff with Gdynia Maritime University, Poland, where he is currently employed as an Associate Professor. His research and teaching interests are mainly in power quality and electrical machines. From 2008 to 2012, he was the Chapter Treasurer/Secretary of the Polish Section, IEEE Instrumentation and Measurement Society.

**JANUSZ MINDYKOWSKI** (Senior Member, IEEE) received the M.Sc. and Ph.D. degrees in electrical engineering from the Gdańsk University of Technology, Poland, in 1974 and 1981, respectively, and the D.Sc. degree from the Warsaw University of Technology, Poland, in 1993. He has been the Head of the Marine Electrical Power Engineering Department, Gdynia Maritime University, since 1994, where he has been a Full Professor, since 2002. His research interests include measurement aspects of technical systems operation and diagnosis, mainly ship's systems. His research is focused on power quality problems and analysis of measurement and monitoring systems in ship technology. From 2008 to 2012, he was the Chapter Chairman of the Polish Section, IEEE Instrumentation and Measurement Society.

**MARCIN PEPLIŃSKI** (Member, IEEE) received the B.Sc., M.Sc., and Ph.D. degrees in electrical engineering from Gdynia Maritime Academy (currently Gdynia Maritime University), Poland, in 1998, 1999, and 2015, respectively. From 1999 to 2001, he has worked as a Telecommunication Engineer. From 2002 to 2003, he was employed on ships as an Electric Assistant. In 2003, he obtained the diploma of Ship Electric Officer. Since 2003, he has been on the staff with Gdynia Maritime University, where he is currently employed as an Assistant Professor. His research and teaching interest includes electrical machines.

**TOMASZ TARASIUK** (Member, IEEE) received the M.S. degree in marine electrical engineering from Gdynia Maritime University, Gdynia, Poland, in 1989, the Ph.D. degree in electrical engineering from the Gdańsk University of Technology, Gdańsk, Poland, in 2001, and the D.S. degree in electrical engineering (metrology and signal processing) from the Warsaw University of Technology, Warsaw, Poland, in 2010. He has been employed by the Gdynia Maritime University, since 1994. His research interests include marine microgrids and power quality assessment.

**JOSE D. COSTA** was born in Lisbon, Portugal. He received the B.S., M.S., and Ph.D. degrees in electrotechnical engineering from the Instituto Superior Técnico, Technical University of Lisbon, in 1996. He currently retired from an Adjunct Professor with the Department of Maritime Engineering, Escola Náutica Infante D. Henrique, Paço de Arcos, Portugal. He is also a Visiting Researcher for those areas in de INOV-INESC Innovation Center, Lisbon. His research interests include systems and control, power semiconductor, and power electronics for SMPS, drives for electrical machinery, and renewable energy applications.

**MÁRIO ASSUNÇÃO** was born in Lisbon, Portugal. He received the B.S. and M.S. degrees in physics engineering from the Universidade Nova de Lisboa, Lisbon, in 1997, and the Ph.D. degree in electrical and computer engineering from the Instituto Superior Técnico (IST), Technical University of Lisbon, Lisbon, in 2015. He is currently an Adjunct Professor with the Department of Maritime Engineering, Escola Náutica Infante D. Henrique, Paço de Arcos, Portugal. His current research interest includes semiconductor and passive elements' modeling.

**LUIS SILVEIRA** was born in Lisbon, Portugal. He received the B.S. and M.S. degrees in electrical engineering from the Instituto Superior de Engenharia de Lisboa, Lisbon, in 1996 and 2007, respectively. He is currently an Assistant Professor with the Department of Maritime Engineering, Escola Náutica Infante D. Henrique, Paço de Arcos, Portugal. His current research interest includes the impact of electric vehicles charging on electrical distribution networks.



**VADYM ZAKHARCHENKO** received the Ph.D. degree, in 1992, and the D.Sc. degree, in 2005. He completed higher education programmes at two higher education institutions—Odessa National Academy of Telecommunication with specialization in automatic telecommunication, in 1985, and National University “Odessa Maritime Academy” with specialization in Ship’s Electrical Equipment and Automation, in 1994. He also completed the Doctorate programme in the field of automation of technological processes in marine transport, in 1991. In 2003, he received the title of a Professor from the Ministry of Education and Science of Ukraine. He also worked as a Ship’s Electro-Technical Officer. Since 1991, he has been on the academic staff of National University “Odessa Maritime Academy”. From 1991 to 2005, he successively held positions of a Lecturer, an Associate Professor, a Professor, and the Dean of the Faculty of Electrical Engineering and Radio-Electronics. Since 2005, he has been holding the position of a Vice-Rector for Scientific and Pedagogical affairs. He is a member of the Ukrainian Association of Electrical Engineers; a Fellow Member of the Institute of Marine Engineering, Science and Technology (IMarEST); a Competent Person of Ukraine to IMO; a member of the Ukrainian National Team of Higher Education Reform Experts. His research interests include ship’s electrical equipment, electronics and control engineering, info-communication technologies, educational and occupational standards, and maritime education and training.

**ALLA DRANKOVA** received the M.Sc. degree in industrial electronics from the Odessa Polytechnic Institute, in 1986, and the Ph.D. degree in automatic control systems and information processing systems from Odessa National Polytechnic University, in 1997. She was employed as an Associate Professor with the Information Systems Department, Odessa National Polytechnic University, from 1998 to 2006. She has been employed by the National University “Odessa Maritime Academy,” since 2006. She currently works as an Associate Professor of the Ship’s Electromechanics and Electrical Engineering Department. Her research and teaching interests are mainly in electrical engineering and automation, intelligent control systems, power quality and energy efficiency solutions. She has been a member of the Ukrainian Association of Electrical Engineers, since 2014.

**MYKOLA MUKHA** (Member, IEEE) received the M.Sc. and Ph.D. degrees in electrical engineering and ships power installations from National University “Odessa Maritime Academy,” in 1975 and 2004, respectively, and the D.Sc. degree in electrotechnical complexes and systems from Lviv Polytechnic National University, in 2018. From 1993 to 2007, he was the First Class Senior Electro-Technical Officer of V. Ships Company. Since 2007, he has been on the staff with National University “Odessa Maritime Academy,” Ukraine. He is currently the head of Ships’ Electromechanics and Electrical Engineering Department, Professor. His research and teaching interests are mainly in electrical engineering and automation, ship power management system and energy efficiency solutions, power quality, electrical machinery, and drives. He has been a member of the Ukrainian Association of Electrical Engineers, since 2014.

**XIAO-YAN XU** was born in Ningbo, Zhejiang, China, in 1970. He received the B.Sc. and M.Sc. degrees in electrical engineering from Shanghai Maritime University, China, in 1993 and 1996, respectively, and the Ph.D. degree in electrical engineering from the Gdańsk University of Technology, Poland, in 2008. Since 1996, he has been on the staff with Shanghai Maritime University, where he is currently employed as a Professor. His research and teaching interests are mainly in power quality and electromagnetic measurement. In 2016, he was elected as the Vice Chairman of the Marine Electrotechnology Committee, China Electrotechnology Society.

...